Anthropogenic warming has increased drought risk in California

Noah S. Diffenbaugh[a,b,1], Daniel L. Swain[a], and Danielle Touma[a]

[a]Department of Environmental Earth System Science and [b]Woods Institute for the Environment, Stanford University, Stanford, CA 94305

California is currently in the midst of a record-setting drought. The drought began in 2012 and now includes the lowest calendar-year and 12-mo precipitation, the highest annual temperature, and the most extreme drought indicators on record. The extremely warm and dry conditions have led to acute water shortages, groundwater overdraft, critically low streamflow, and enhanced wildfire risk. Analyzing historical climate observations from California, we find that precipitation deficits in California were more than twice as likely to yield drought years if they occurred when conditions were warm. We find that although there has not been a substantial change in the probability of either negative or moderately negative precipitation anomalies in recent decades, the occurrence of drought years has been greater in the past two decades than in the preceding century. In addition, the probability that precipitation deficits co-occur with warm conditions and the probability that precipitation deficits produce drought have both increased. Climate model experiments with and without anthropogenic forcings reveal that human activities have increased the probability that dry precipitation years are also warm. Further, a large ensemble of climate model realizations reveals that additional global warming over the next few decades is very likely to create ~100% probability that any annual-scale dry period is also extremely warm. We therefore conclude that anthropogenic warming is increasing the probability of co-occurring warm–dry conditions like those that have created the acute human and ecosystem impacts associated with the "exceptional" 2012–2014 drought in California.

drought | climate extremes | climate change detection | event attribution | CMIP5

The state of California is the largest contributor to the economic and agricultural activity of the United States, accounting for a greater share of population (12%) (1), gross domestic product (12%) (2), and cash farm receipts (11%) (3) than any other state. California also includes a diverse array of marine and terrestrial ecosystems that span a wide range of climatic tolerances and together encompass a global biodiversity "hotspot" (4). These human and natural systems face a complex web of competing demands for freshwater (5). The state's agricultural sector accounts for 77% of California water use (5), and hydroelectric power provides more than 9% of the state's electricity (6). Because the majority of California's precipitation occurs far from its urban centers and primary agricultural zones, California maintains a vast and complex water management, storage, and distribution/conveyance infrastructure that has been the focus of nearly constant legislative, legal, and political battles (5). As a result, many riverine ecosystems depend on mandated "environmental flows" released by upstream dams, which become a point of contention during critically dry periods (5).

California is currently in the midst of a multiyear drought (7). The event encompasses the lowest calendar-year and 12-mo precipitation on record (8), and almost every month between December 2011 and September 2014 exhibited multiple indicators of drought (Fig. S1). The proximal cause of the precipitation deficits was the recurring poleward deflection of the cool-season storm track by a region of persistently high atmospheric pressure,

which steered Pacific storms away from California over consecutive seasons (8–11). Although the extremely persistent high pressure is at least a century-scale occurrence (8), anthropogenic global warming has very likely increased the probability of such conditions (8, 9).

Despite insights into the causes and historical context of precipitation deficits (8–11), the influence of historical temperature changes on the probability of individual droughts has—until recently—received less attention (12–14). Although precipitation deficits are a prerequisite for the moisture deficits that constitute "drought" (by any definition) (15), elevated temperatures can greatly amplify evaporative demand, thereby increasing overall drought intensity and impact (16, 17). Temperature is especially important in California, where water storage and distribution systems are critically dependent on winter/spring snowpack, and excess demand is typically met by groundwater withdrawal (18–20). The impacts of runoff and soil moisture deficits associated with warm temperatures can be acute, including enhanced wildfire risk (21), land subsidence from excessive groundwater withdrawals (22), decreased hydropower production (23), and damage to habitat of vulnerable riparian species (24).

Recent work suggests that the aggregate combination of extremely high temperatures and very low precipitation during the 2012–2014 event is the most severe in over a millennium (12). Given the known influence of temperature on drought, the fact that the 2012–2014 record drought severity has co-occurred with record statewide warmth (7) raises the question of whether long-term warming has altered the probability that precipitation deficits yield extreme drought in California.

Significance

California ranks first in the United States in population, economic activity, and agricultural value. The state is currently experiencing a record-setting drought, which has led to acute water shortages, groundwater overdraft, critically low streamflow, and enhanced wildfire risk. Our analyses show that California has historically been more likely to experience drought if precipitation deficits co-occur with warm conditions and that such confluences have increased in recent decades, leading to increases in the fraction of low-precipitation years that yield drought. In addition, we find that human emissions have increased the probability that low-precipitation years are also warm, suggesting that anthropogenic warming is increasing the probability of the co-occurring warm–dry conditions that have created the current California drought.

SUSTAINABILITY SCIENCE

Results

We analyze the "Palmer" drought metrics available from the US National Climatic Data Center (NCDC) (25). The NCDC Palmer metrics are based on the Palmer Drought Severity Index (PDSI), which uses monthly precipitation and temperature to calculate moisture balance using a simple "supply-and-demand" model (26) (*Materials and Methods*). We focus on the Palmer Modified Drought Index (PMDI), which moderates transitions between wet and dry periods (compared with the PDSI) (27). However, we note that the long-term time series of the PMDI is similar to that of other Palmer drought indicators, particularly at the annual scale (Figs. S1 and S2).

Because multiple drought indicators reached historic lows in July 2014 (Figs. S1–S3), we initially focus on statewide PMDI, temperature, and precipitation averaged over the August–July 12-mo period. We find that years with a negative PMDI anomaly exceeding –1.0 SDs (hereafter "1-SD drought") have occurred approximately twice as often in the past two decades as in the preceding century (six events in 1995–2014 = 30% of years; 14 events in 1896–1994 = 14% of years) (Fig. 1*A* and Fig. S4). This increase in the occurrence of 1-SD drought years has taken place without a substantial change in the probability of negative precipitation anomalies (53% in 1896–2014 and 55% in 1995–2014) (Figs. 1*B* and 2 *A* and *B*). Rather, the observed doubling of the occurrence of 1-SD drought years has coincided with a doubling of the frequency with which a negative precipitation year produces a 1-SD drought, with 55% of negative precipitation years in 1995–2014 co-occurring with a –1.0 SD PMDI anomaly, compared with 27% in 1896–1994 (Fig. 1 *A* and *B*).

Most 1-SD drought years have occurred when conditions were both dry (precipitation anomaly < 0) and warm (temperature anomaly > 0), including 15 of 20 1-SD drought years during 1896–2014 (Fig. 2*A* and Fig. S4) and 6 of 6 during 1995–2014 (Fig. 2*B* and Fig. S4). Similarly, negative precipitation anomalies are much more likely to produce 1-SD drought if they co-occur with a positive temperature anomaly. For example, of the 63 negative precipitation years during 1896–2014, 15 of the 32 warm–dry years (47%) produced 1-SD drought, compared with only 5 of the 31 cool–dry years (16%) (Fig. 2*A*). (During 1896–1994, 41% of warm–dry years produced 1-SD droughts, compared with 17% of cool–dry years.) The probability that a negative precipitation anomaly co-occurs with a positive temperature anomaly has increased recently, with warm–dry years occurring more than twice as often in the past two decades (91%) as in the preceding century (42%) (Fig. 1*B*).

All 20 August–July 12-mo periods that exhibited a –1.0 SD PMDI anomaly also exhibited a –0.5 SD precipitation anomaly (Fig. 1*B* and 2*E*), suggesting that moderately low precipitation is prerequisite for a 1-SD drought year. However, the occurrence of –0.5 SD precipitation anomalies has not increased in recent years (40% in 1896–2014 and 40% in 1995–2014) (Fig. 2 *A* and *B*). Rather, these moderate precipitation deficits have been far more likely to produce 1-SD drought when they occur in a warm year. For example, during 1896–2014, 1-SD drought occurred in 15 of the 28 years (54%) that exhibited both a –0.5 SD precipitation anomaly and a positive temperature anomaly, but in only 5 of the 20 years (25%) that exhibited a –0.5 SD precipitation anomaly and a negative temperature anomaly (Fig. 2*A*). During 1995–2014, 6 of the 8 moderately dry years produced 1-SD drought (Fig. 1*A*), with all 6 occurring in years in which the precipitation anomaly exceeded –0.5 SD and the temperature anomaly exceeded 0.5 SD (Fig. 1*C*).

Taken together, the observed record from California suggests that (*i*) precipitation deficits are more likely to yield 1-SD PMDI droughts if they occur when conditions are warm and (*ii*) the occurrence of 1-SD PMDI droughts, the probability of precipitation deficits producing 1-SD PMDI droughts, and the probability of precipitation deficits co-occurring with warm conditions have all been greater in the past two decades than in the preceding century.

These increases in drought risk have occurred despite a lack of substantial change in the occurrence of low or moderately low precipitation years (Figs. 1*B* and 2 *A* and *B*). In contrast, statewide warming (Fig. 1*C*) has led to a substantial increase in warm conditions, with 80% of years in 1995–2014 exhibiting a positive temperature anomaly (Fig. 2*B*), compared with 45% of years in 1896–2014 (Fig. 2*A*). As a result, whereas 58% of moderately dry years were warm during 1896–2014 (Fig. 2*A*) and 50% were warm during 1896–1994, 100% of the 8 moderately dry years in 1995–2014 co-occurred with a positive temperature anomaly (Fig. 2*B*). The observed statewide warming (Fig. 1*C*) has therefore substantially increased the probability that when moderate precipitation deficits occur, they occur during warm years.

The recent statewide warming clearly occurs in climate model simulations that include both natural and human forcings ("Historical" experiment), but not in simulations that include only natural forcings ("Natural" experiment) (Fig. 3*B*). In particular, the Historical and Natural temperatures are found to be different at the 0.001 significance level during the most recent 20-, 30-, and 40-y periods of the historical simulations (using the block bootstrap resampling applied in ref. 28). In contrast, although the Historical experiment exhibits a slightly higher mean annual precipitation (0.023 significance level), there is no statistically

August-July 12-month Mean
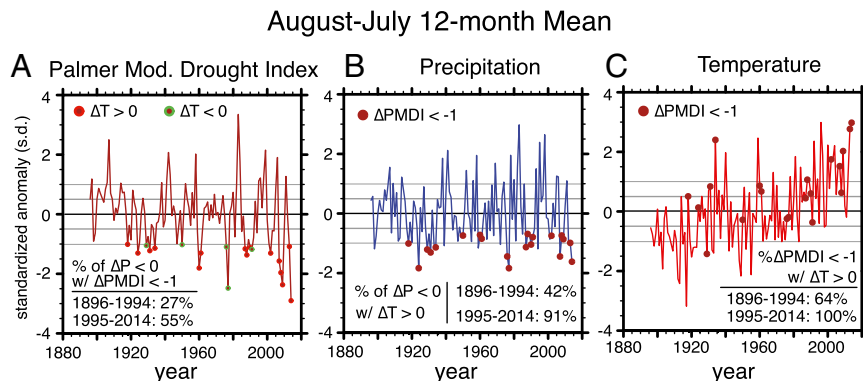
Fig. 1. Historical time series of drought (*A*), precipitation (*B*), and temperature (*C*) in California. Values are calculated for the August–July 12-mo mean in each year of the observed record, beginning in August 1895. In each year, the standardized anomaly is expressed as the magnitude of the anomaly from the long-term annual mean, divided by the SD of the detrended historical annual anomaly time series. The PMDI is used as the primary drought indicator, although the other Palmer indicators exhibit similar historical time series (Figs. S1 and S2). Circles show the years in which the PMDI exhibited a negative anomaly exceeding –1.0 SDs, which are referred to as 1-SD drought years in the text.
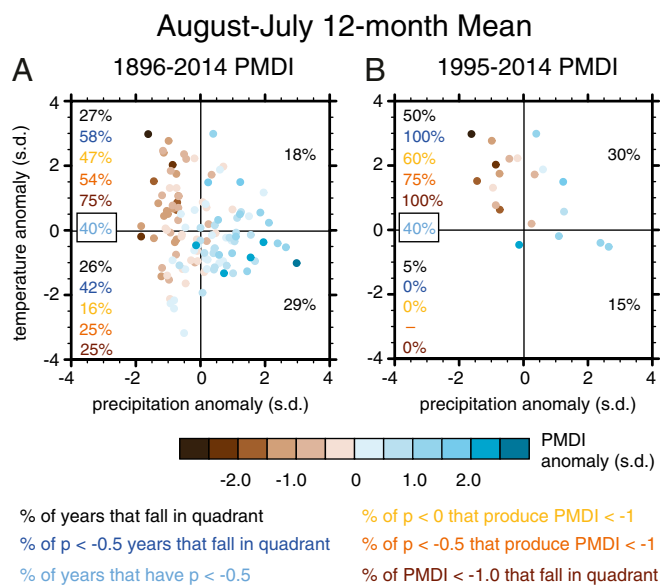
Fig. 2. Historical occurrence of drought, precipitation, and temperature in California. Standardized anomalies are shown for each August–July 12-mo period in the historical record (calculated as in Fig. 1). Anomalies are shown for the full historical record (A) and for the most recent two decades (B). Percentage values show the percentage of years meeting different precipitation and drought criteria that fall in each quadrant of the temperature–precipitation space. The respective criteria are identified by different colors of text.
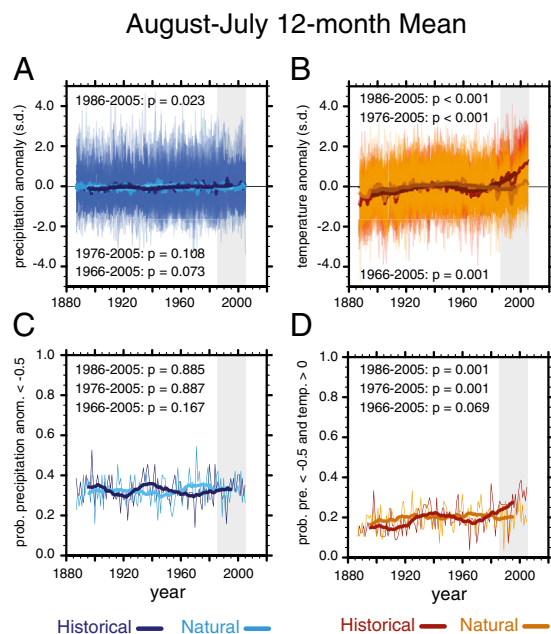
risk that any negative—or extremely negative—12-mo precipitation anomaly is also extremely warm.

The overall occurrence of dry years declines after ~2040 (Fig. 4C). However, the occurrence of extreme 12-mo precipitation deficits (–1.5 SD) is greater in 2006–2080 than in 1920–2005 (<0.03 significance level). This detectable increase in extremely low-precipitation years adds to the effect of rising temperatures and contributes to the increasing occurrence of extremely warm–dry 12-mo periods during the 21st century.

All four 3-mo seasons likewise show higher probability of co-occurring 1.5 SD warm–dry anomalies after ~1980, with the probability of an extremely warm–dry season equaling that of an extremely dry season by ~2030 for spring, summer, and autumn, and by ~2060 for winter (Fig. 4D). In addition, the probability of a –1.5 SD precipitation anomaly increases in spring ($P < 0.001$) and autumn ($P = 0.01$) in 2006–2080 relative to 1920–2005, with spring occurrence increasing by ~75% and autumn occurrence increasing by ~44%—which represents a substantial and statistically significant increase in the risk of extremely low-precipitation events at both margins of California's wet season. In contrast, there is no statistically significant difference in the probability of a –1.5 SD precipitation anomaly for winter.

Discussion

A recent report by Seager et al. (30) found no significant long-term trend in cool-season precipitation in California during the 20th and early 21st centuries, which is consistent with our

significant difference in probability of a –0.5 SD precipitation anomaly (Fig. 3 A and C). However, the Historical experiment exhibits greater probability of a –0.5 SD precipitation anomaly co-occurring with a positive temperature anomaly (0.001 significance level) (Fig. 3D), suggesting that human forcing has caused the observed increase in probability that moderately dry precipitation years are also warm.

The fact that the occurrence of warm and moderately dry years approaches that of moderately dry years in the last decades of the Historical experiment (Fig. 3 B and C) and that 91% of negative precipitation years in 1995–2014 co-occurred with warm anomalies (Fig. 1B) suggests possible emergence of a regime in which nearly all dry years co-occur with warm conditions. We assess this possibility using an ensemble of 30 realizations of a single global climate model [the National Center for Atmospheric Research (NCAR) Community Earth System Model (CESM1) Large Ensemble experiment ("LENS")] (29) (*Materials and Methods*). Before ~1980, the simulated probability of a warm–dry year is approximately half that of a dry year (Fig. 4B), similar to observations (Figs. 1B and 2). However, the simulated probability of a warm–dry year becomes equal to that of a dry year by ~2030 of RCP8.5. Likewise, the probabilities of co-occurring 0.5, 1.0 and 1.5 SD warm–dry anomalies become approximately equal to those of 0.5, 1.0, and 1.5 SD dry anomalies (respectively) by ~2030 (Fig. 4B).

The probability of co-occurring extremely warm and extremely dry conditions (1.5 SD anomaly) remains greatly elevated throughout the 21st century (Fig. 4B). In addition, the number of multiyear periods in which a –0.5 SD precipitation anomaly co-occurs with a 0.5 SD temperature anomaly more than doubles between the Historical and RCP8.5 experiments (Fig. 4A). We find similar results using a 12-mo moving average (Fig. 4C). As with the August–July 12-mo mean (Fig. 4B), the probability of a dry year is approximately twice the probability of a warm–dry year for all 12-mo periods before ~1980 (Fig. 4C). However, the occurrence of warm years (including +1.5 SD temperature anomalies) increases after ~1980, reaching 1.0 by ~2030. This increase implies a transition to a permanent condition of ~100%

Fig. 3. Influence of anthropogenic forcing on the probability of warm–dry years in California. Temperature and precipitation values are calculated for the August–July 12-mo mean in each year of the CMIP5 Historical and Natural forcing experiments (*Materials and Methods*). The *Top* panels (A and B) show the time series of ensemble–mean standardized temperature and precipitation anomalies. The *Bottom* panels (C and D) show the unconditional probability (across the ensemble) that the annual precipitation anomaly is less than –0.5 SDs, and the conditional probability that both the annual precipitation anomaly is less than –0.5 SDs and the temperature anomaly is greater than 0. The bold curves show the 20-y running mean of each annual time series. The CMIP5 Historical and Natural forcing experiments were run until the year 2005. *P* values are shown for the difference between the Historical and Natural experiments for the most recent 20-y (1986–2005; gray band), 30-y (1976–2005), and 40-y (1966–2005) periods of the CMIP5 protocol. *P* values are calculated using the block bootstrap resampling approach of ref. 28 (*Materials and Methods*).
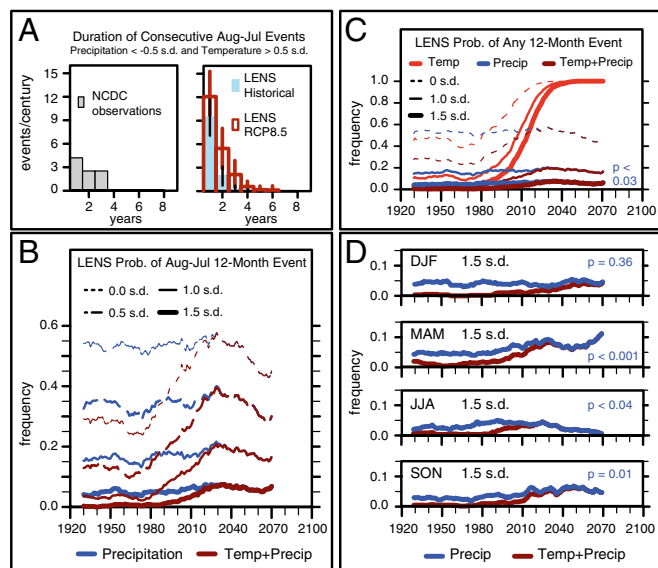
Fig. 4. Projected changes in the probability of co-occurring warm–dry conditions in the 21st century. (*A*) Histogram of the frequency of occurrence of consecutive August–July 12-mo periods in which the 12-mo precipitation anomaly is less than –0.5 SDs and the 12-mo temperature anomaly is at least 0.5 SDs, in historical observations and the LENS large ensemble experiment. (*B*) The probability that a negative 12-mo precipitation anomaly and a positive 12-mo temperature anomaly equal to or exceeding a given magnitude occur in the same August–July 12-mo period, for varying severity of anomalies. (*C*) The probability that a negative precipitation anomaly and a positive temperature anomaly equal to or exceeding a given magnitude occur in the same 12-mo period, for all possible 12-mo periods (using a 12-mo running mean; see *Materials and Methods*), for varying severity of anomalies. (*D*) The unconditional probability of a –1.5 SD seasonal precipitation anomaly (blue curve) and the conditional probability that a –1.5 SD seasonal precipitation anomaly occurs in conjunction with a 1.5 SD seasonal temperature anomaly (red curve), for each of the four 3-mo seasons. Time series show the 20-y running mean of each annual time series. *P* values are shown for the difference in occurrence of –1.5 SD precipitation anomalies between the Historical period (1920–2005) and the RCP8.5 period (2006–2080).

findings. Further, under a scenario of strongly elevated greenhouse forcing, Neelin et al. (31) found a modest increase in California mean December–January–February (DJF) precipitation associated with a local eastward extension of the mean subtropical jet stream west of California. However, considerable evidence (8–11, 31–33) simultaneously suggests that the response of northeastern Pacific atmospheric circulation to anthropogenic warming is likely to be complex and spatiotemporally inhomogeneous, and that changes in the atmospheric mean state may not be reflective of changes in the risk of extreme events (including atmospheric configurations conducive to precipitation extremes). Although there is clearly value in understanding possible changes in precipitation, our results highlight the fact that efforts to understand drought without examining the role of temperature miss a critical contributor to drought risk. Indeed, our results show that even in the absence of trends in mean precipitation—or trends in the occurrence of extremely low-precipitation events—the risk of severe drought in California has already increased due to extremely warm conditions induced by anthropogenic global warming.

We note that the interplay between the existence of a well-defined summer dry period and the historical prevalence of a substantial high-elevation snowpack may create particular susceptibility to temperature-driven increases in drought duration and/or intensity in California. In regions where precipitation exhibits a distinct seasonal cycle, recovery from preexisting drought conditions is unlikely during the characteristic yearly dry spell (34). Because California's dry season occurs during the warm

summer months, soil moisture loss through evapotranspiration (ET) is typically high—meaning that soil moisture deficits that exist at the beginning of the dry season are exacerbated by the warm conditions that develop during the dry season, as occurred during the summers of 2013 and 2014 (7).

Further, California's seasonal snowpack (which resides almost entirely in the Sierra Nevada Mountains) provides a critical source of runoff during the low-precipitation spring and summer months. Trends toward earlier runoff in the Sierra Nevada have already been detected in observations (e.g., ref. 35), and continued global warming is likely to result in earlier snowmelt and increased rain-to-snow ratios (35, 36). As a result, the peaks in California's snowmelt and surface runoff are likely to be more pronounced and to occur earlier in the calendar year (35, 36), increasing the duration of the warm-season low-runoff period (36) and potentially reducing montane surface soil moisture (37). Although these hydrological changes could potentially increase soil water availability in previously snow-covered regions during the cool low-ET season (34), this effect would likely be outweighed by the influence of warming temperatures (and decreased runoff) during the warm high-ET season (36, 38), as well as by the increasing occurrence of consecutive years with low precipitation and high temperature (Fig. 4*A*).

The increasing risk of consecutive warm–dry years (Fig. 4*A*) raises the possibility of extended drought periods such as those found in the paleoclimate record (14, 39, 40). Recent work suggests that record warmth could have made the current event the most severe annual-scale drought of the past millennium (12). However, numerous paleoclimate records also suggest that the region has experienced multidecadal periods in which most years were in a drought state (14, 39, 41, 42), albeit less acute than the current California event (12, 39, 41). Although multidecadal ocean variability was a primary cause of the megadroughts of the last millenium (41), the emergence of a condition in which there is ~100% probability of an extremely warm year (Fig. 4) substantially increases the risk of prolonged drought conditions in the region (14, 39, 40).

A number of caveats should be considered. For example, ours is an implicit approach that analyzes the temperature and precipitation conditions that have historically occurred with low PMDI years, but does not explicitly explore the physical processes that produce drought. The impact of increasing temperatures on the processes governing runoff, baseflow, groundwater, soil moisture, and land-atmosphere evaporative feedbacks over both the historical period and in response to further global warming remains a critical uncertainty (43). Likewise, our analyses of anthropogenic forcing rely on global climate models that do not resolve the topographic complexity that strongly influences California's precipitation and temperature. Further investigation using high-resolution modeling approaches that better resolve the boundary conditions and fine-scale physical processes (44–46) and/or using analyses that focus on the underlying large-scale climate dynamics of individual extreme events (8) could help to overcome the limitations of simulated precipitation and temperature in the current generation of global climate models.

Conclusions

Our results suggest that anthropogenic warming has increased the probability of the co-occurring temperature and precipitation conditions that have historically led to drought in California. In addition, continued global warming is likely to cause a transition to a regime in which essentially every seasonal, annual, and multiannual precipitation deficit co-occurs with historically warm conditions. The current warm–dry event in California—as well as historical observations of previous seasonal, annual, and multiannual warm–dry events—suggests such a regime would substantially increase the risk of severe impacts on human and natural systems. For example, the projected increase in extremely

low precipitation and extremely high temperature during spring and autumn has substantial implications for snowpack water storage, wildfire risk, and terrestrial ecosystems (47). Likewise, the projected increase in annual and multiannual warm–dry periods implies increasing risk of the acute water shortages, critical groundwater overdraft, and species extinction potential that have been experienced during the 2012–2014 drought (5, 20).

California's human population (38.33 million as of 2013) has increased by nearly 72% since the much-remembered 1976–1977 drought (1). Gains in urban and agricultural water use efficiency have offset this rapid increase in the number of water users to the extent that overall water demand is nearly the same in 2013 as it was in 1977 (5). As a result, California's per capita water use has declined in recent decades, meaning that additional short-term water conservation in response to acute shortages during drought conditions has become increasingly challenging. Although a variety of opportunities exist to manage drought risk through long-term changes in water policy, management, and infrastructure (5), our results strongly suggest that global warming is already increasing the probability of conditions that have historically created high-impact drought in California.

Materials and Methods

We use historical time series of observed California statewide temperature, precipitation, and drought data from the National Oceanic and Atmospheric Administration's NCDC (7). The data are from the NCDC "nClimDiv" divisional temperature–precipitation–drought database, available at monthly time resolution from January 1895 to the present (7, 25). The NCDC nClimDiv database includes temperature, precipitation, and multiple Palmer drought indicators, aggregated at statewide and substate climate division levels for the United States. The available Palmer drought indicators include PDSI, the Palmer Hydrological Drought Index (PHDI), and PMDI.

PMDI and PHDI are variants of PDSI (25–27, 48, 49). PDSI is an index that measures the severity of wet and dry anomalies (26). The NCDC nClimDiv PDSI calculation is reported at the monthly scale, based on monthly temperature and precipitation (49). Together, the monthly temperature and precipitation values are used to compute the net moisture balance, based on a simple supply-and-demand model that uses potential evapotranspiration (PET) calculated using the Thornthwaite method. Calculated PET values can be very different when using other methods (e.g., Penman–Monteith), with the Thornthwaite method's dependence on surface temperature creating the potential for overestimation of PET (e.g., ref. 43). However, it has been found that the choice of methods in the calculation of PET does not critically influence the outcome of historical PDSI estimates in the vicinity of California (15, 43, 50). In contrast, the sensitivity of the PET calculation to large increases in temperature could make the PDSI inappropriate for calculating the response of drought to high levels of greenhouse forcing (15). As a result, we analyze the NCDC Palmer indicators in conjunction with observed temperature and precipitation data for the historical period, but we do not calculate the Palmer indicators for the future (for future projections of the PDSI, refer to refs. 15 and 40).

Because the PDSI is based on recent temperature and precipitation conditions (and does not include human demand for water), it is considered an indicator of "meterological" drought (25). The PDSI calculates "wet," "dry," and "transition" indices, using the wet or dry index when the probability is 100% and the transition index when the probability is less than 100% (26). Because the PMDI always calculates a probability-weighted average of the wet and dry indices (27), the PDSI and PMDI will give equal values in periods that are clearly wet or dry, but the PMDI will yield smoother transitions between wet and dry periods (25). In this work, we use the PMDI as our primary drought indicator, although we note that the long-term time series of the PMDI is similar to that of the PDSI and PHDI, particularly at the annual scale considered here (Figs. S1 and S2).

We analyze global climate model simulations from phase 5 of the Coupled Model Intercomparison Project (CMIP5) (51). We compare two of the CMIP5 multimodel historical experiments (which were run through 2005): (i) the Historical experiment, in which the climate models are prescribed both anthropogenic and nonanthropogenic historical climate forcings, and (ii) the Natural experiment, in which the climate models are prescribed only the nonanthropogenic historical climate forcings. We analyze those realizations for which both temperature and precipitation were available from both experiments at the time of data acquisition. We calculate the temperature and precipitation values over the state of California at each model's native

resolution using all grid points that overlap with the geographical borders of California, as defined by a high-resolution shapefile (vector digital data obtained from the US Geological Survey via the National Weather Service at www.nws.noaa.gov/geodata/catalog/national/html/us_state.htm).

We also analyze NCAR's large ensemble ("LENS") climate model experiment (29). The LENS experiment includes 30 realizations of the NCAR CESM1. This large single-model experiment enables quantification of the uncertainty arising from internal climate system variability. Although the calculation of this "irreducible" uncertainty likely varies between climate models, it exists independent of uncertainty arising from model structure, model parameter values, and climate forcing pathway. At the time of acquisition, LENS results were available for 1920–2005 in the Historical experiment and 2006–2080 in the RCP8.5 (Representative Concentration Pathway) experiment. The four RCPs are mostly indistinguishable over the first half of the 21st century (52). RCP8.5 has the highest forcing in the second half of the 21st century and reaches ~4 °C of global warming by the year 2100 (52).

Given that the ongoing California drought encompasses the most extreme 12-mo precipitation deficit on record (8) and that both temperature and many drought indicators reached their most extreme historical values for California in July 2014 (7) (Fig. 1 and Figs. S1 and S2), we use the 12-mo August–July period as one period of analysis. However, because severe conditions can manifest at both multiannual and subannual timescales, we also analyze the probability of occurrence of co-occurring warm and dry conditions for multiannual periods, for all possible 12-mo periods, and for the winter (DJF), spring (March–April–May), summer (June–July–August), and autumn (September–October–November) seasons.

We use the monthly-mean time series from NCDC to calculate observed time series of statewide 12-mo values of temperature, precipitation, and PMDI. Likewise, we use the monthly-mean time series from CMIP5 and LENS to calculate simulated time series of statewide 12-mo and seasonal values of temperature and precipitation. From the time series of annual-mean values for each observed or simulated realization, we calculate (i) the baseline mean value over the length of the record, (ii) the annual anomaly from the baseline mean value, (iii) the SD of the detrended baseline annual anomaly time series, and (iv) the ratio of each individual annual anomaly value to the SD of the detrended baseline annual anomaly time series. (For the 21st-century simulations, we use the Historical simulation as the baseline.) Our time series of standardized values are thereby derived from the time series of 12-mo annual (or 3-mo seasonal) mean anomaly values that occur in each year.

For the multiannual analysis, we calculate consecutive occurrences of August–July 12-mo values. For the analysis of all possible 12-mo periods, we generate the annual time series of each 12-mo period (January–December, February–January, etc.) using a 12-mo running mean. For the seasonal analysis, we generate the time series by calculating the mean of the respective 3-mo season in each year.

We quantify the statistical significance of differences in the populations of different time periods using the block bootstrap resampling approach of ref. 28. For the CMIP5 Historical and Natural ensembles, we compare the populations of the August–July values in the two experiments for the 1986–2005, 1976–2005, and 1966–2005 periods. For the LENS seasonal analysis, we compare the respective populations of DJF, March–April–May, June–July–August, and September–October–November values in the 1920–2005 and 2006–2080 periods. For the LENS 12-mo analysis, we compare the populations of 12-mo values in the 1920–2005 and 2006–2080 periods, testing block lengths up to 16 to account for temporal autocorrelation out to 16 mo for the 12-mo running mean data. (Autocorrelations beyond 16 mo are found to be negligible.)

Throughout the text, we consider drought to be those years in which negative 12-mo PMDI anomalies exceed –1.0 SDs of the historical interannual PMDI variability. We stress that this value is indicative of the variability of the annual (12-mo) PMDI, rather than of the monthly values (compare Fig. 1 and Figs. S1 and S2). We consider "moderate" temperature and precipitation anomalies to be those that exceed 0.5 SDs ("0.5 SD") and "extreme" temperature and precipitation anomalies to be those that exceed 1.5 SDs ("1.5 SD").

1. US Census Bureau (2014) *State and County QuickFacts*. Available at quickfacts.census. gov/qfd/states/06000.html.
2. US Bureau of Economic Analysis (2014) *Bureau of Economic Analysis Interactive Data*. Available at www.bea.gov/.
3. US Department of Agriculture (2013) *CALIFORNIA Agricultural Statistics 2012 Crop Year*. Available at www.nass.usda.gov/Statistics_by_State/California/Publications/ California_Ag_Statistics/Reports/2012cas-all.pdf.
4. Myers N, Mittermeier RA, Mittermeier CG, da Fonseca GAB, Kent J (2000) Biodiversity hotspots for conservation priorities. *Nature* 403(6772):853–858.
5. Hanak E, et al. (2011) *Managing California's Water: From Conflict to Reconciliation* (Public Policy Institute of California, San Francisco).
6. California Energy Commission (2014) *California Energy Almanac*. Available at www. energyalmanac.ca.gov/.
7. US National Climate Data Center (2014) *National Climate Data Center NNDC Climate Data Online*. Available at www7.ncdc.noaa.gov/CDO/CDODivisionalSelect.jsp.
8. Swain DL, et al. (2014) The extraordinary California drought of 2013-2014: Character, context, and the role of climate change. *Bull Am Meteorol Soc* 95(7):S3–S7.
9. Wang S, Hipps L, Gillies RR, Yoon J (2014) Probable causes of the abnormal ridge accompanying the 2013–2014 California drought: ENSO precursor and anthropogenic warming footprint. *Geophys Res Lett* 41(9):3220–3226.
10. Wang H, Schubert S (2014) Causes of the extreme dry conditions over California during early 2013. *Bull Am Meteorol Soc* 95(7):S7–S11.
11. Funk C, Hoell A, Stone D (2014) Examining the contribution of the observed global warming trend to the California droughts of 2012/13 and 2013/2014. *Bull Am Meteorol Soc* 95(7):S11–S15.
12. Griffin D, Anchukaitis KJ (2014) How unusual is the 2012-2014 California drought? *Geophys Res Lett* 41(24):9017–9023.
13. AghaKouchak A, Cheng L, Mazdiyasni O, Farahmand A (2014) Global warming and changes in risk of concurrent climate extremes: Insights from the 2014 California drought. *Geophys Res Lett* 41(24):8847–8852.
14. Overpeck JT (2013) Climate science: The challenge of hot drought. *Nature* 503(7476): 350–351.
15. Dai A (2010) Drought under global warming: A review. *Wiley Interdiscip Rev Clim Chang* 2(1):45–65.
16. Dai A (2013) Increasing drought under global warming in observations and models. *Nat Clim Chang* 3(1):52–58.
17. Dai A, Trenberth KE, Qian T (2004) A global dataset of Palmer Drought Severity Index for 1870-2002: Relationship with soil moisture and effects of surface warming. *J Hydrometeorol* 5(6):1117–1130.
18. Famiglietti JS, et al. (2011) Satellites measure recent rates of groundwater depletion in California's Central Valley. *Geophys Res Lett* 38(3):L03403.
19. Borsa AA, Agnew DC, Cayan DR (2014) Remote hydrology. Ongoing drought-induced uplift in the western United States. *Science* 345(6204):1587–1590.
20. Christian-Smith J, Levy M, Gleick P (2014) Maladaptation to drought: A case report from California. *Sustain Sci*, 10.1007/s11625-014-0269-1.
21. Westerling AL, Hidalgo HG, Cayan DR, Swetnam TW (2006) Warming and earlier spring increase western U.S. forest wildfire activity. *Science* 313(5789):940–943.
22. King NE, et al. (2007) Space geodetic observation of expansion of the San Gabriel Valley, California, aquifer system, during heavy rainfall in winter 2004–2005. *J Geophys Res Solid Earth* 112(3):B03409.
23. US Energy Information Administration (2014) California drought leads to less hydropower, increased natural gas generation. *Today in Energy*. Available at www.eia. gov/todayinenergy/detail.cfm?id=182.
24. Palmer MA, et al. (2009) Climate change and river ecosystems: Protection and adaptation options. *Environ Manage* 44(6):1053–1068.
25. US National Climate Data Center (2014) *nClimDiv STATEWIDE-REGIONAL-NATIONAL DROUGHT*. Available at ftp://ftp.ncdc.noaa.gov/pub/data/cirs/climdiv/drought-readme.txt.
26. Palmer WC (1965) *Meteorological Drought* (US Department of Commerce, Weather Bureau, Washington, DC).
27. Heddinghaus TR, Sabol P (1991) in *Proceedings of the Seventh Conference on Applied Climatology* (American Meteorological Society, Boston).
28. Singh D, Tsiang M, Rajaratnam B, Diffenbaugh NS (2014) Observed changes in extreme wet and dry spells during the South Asian summer monsoon season. *Nat Clim Chang* 4(6):456–461.

29. Kay JE, et al. (2015) The Community Earth System Model (CESM) large ensemble project: A community resource for studying climate change in the presence of internal climate variability. *Bull Am Meteorol Soc*, 10.1175/BAMS-D-13-00255.1.
30. Seager R, et al. (2014) *Causes and Predictability of the 2011-14 California Drought*. Available at cpo.noaa.gov/sites/cpo/MAPP/Task%20Forces/DTF/californiadrought/ california_drought_report.pdf.
31. Neelin JD, Langenbrunner B, Meyerson JE, Hall A, Berg N (2013) California winter precipitation change under global warming in the Coupled Model Intercomparison Project Phase 5 Ensemble. *J Clim* 26(17):6238–6256.
32. Seager R, et al. (2014) Dynamical and thermodynamical causes of large-scale changes in the hydrological cycle over North America in response to global warming. *J Clim* 27(17):7921–7948.
33. Simpson IR, Shaw TA, Seager R (2014) A diagnosis of the seasonally and longitudinally varying midlatitude circulation response to global warming. *J Atmos Sci* 71(7): 2489–2515.
34. Van Loon AF, et al. (2014) How climate seasonality modifies drought duration and deficit. *J Geophys Res Atmos* 119(8):4640–4656.
35. Rauscher SA, Pal JS, Diffenbaugh NS, Benedetti MM (2008) Future changes in snowmelt-driven runoff timing over the western US. *Geophys Res Lett* 35(16):L16703.
36. Ashfaq M, et al. (2013) Near-term acceleration of hydroclimatic change in the western U.S. *J Geophys Res* 118(10):10,676–10,693.
37. Blankinship JC, Meadows MW, Lucas RG, Hart SC (2014) Snowmelt timing alters shallow but not deep soil moisture in the Sierra Nevada. *Water Resour Res* 50(2):1448–1456.
38. Diffenbaugh NS, Ashfaq M (2010) Intensification of hot extremes in the United States. *Geophys Res Lett* 37(15):L15701.
39. Ault TR, Cole JE, Overpeck JT, Pederson GT, Meko DM (2014) Assessing the risk of persistent drought using climate model simulations and paleoclimate data. *J Clim* 27(20):7529–7549.
40. Cook BI, Ault TR, Smerdon JE (2015) Unprecedented 21st century drought risk in the American Southwest and Central Plains. *Science Advances* 1(1):e1400082.
41. Cook BI, Smerdon JE, Seager R, Cook ER (2013) Pan-continental droughts in North America over the last millennium. *J Clim* 27(1):383–397.
42. Cook BI, Seager R, Smerdon JE (2014) The worst North American drought year of the last millennium: 1934. *Geophys Res Lett* 41(20):7298–7305.
43. Sheffield J, Wood EF, Roderick ML (2012) Little change in global drought over the past 60 years. *Nature* 491(7424):435–438.
44. Diffenbaugh NS, Pal JS, Trapp RJ, Giorgi F (2005) Fine-scale processes regulate the response of extreme events to global climate change. *Proc Natl Acad Sci USA* 102(44): 15774–15778.
45. Diffenbaugh NS, Ashfaq M, Scherer M (2011) Transient regional climate change: Analysis of the summer climate response in a high-resolution, century-scale, ensemble experiment over the continental United States. *J Geophys Res* 116(D24):D24111.
46. Lebassi-Habtezion B, Diffenbaugh NS (2013) Nonhydrostatic nested climate modeling: A case study of the 2010 summer season over the western United States. *J Geophys Res Atmos* 118(19):10944–10962.
47. Romero-Lankao P, et al. (2014) Impacts, adaptation, and vulnerability. Part B: Regional aspects. Contribution of working group II to the Fifth Assessment Report of the Intergovernmental Panel of Climate Change. *Climate Change*, eds Barros VR, et al. (Cambridge Univ Press, Cambridge, UK), pp 1439–1498.
48. Heim RR, Jr (2002) A review of twentieth-century drought indices used in the United States. *Bull Am Meteorol Soc* 83(8):1149–1165.
49. Karl TR (1986) The sensitivity of the Palmer drought severity index and Palmer's Z-index to their calibration coefficients including potential evapotranspiration. *J Clim Appl Meteorol* 25(1):77–86.
50. Van der Schrier G, Jones PD, Briffa KR (2011) The sensitivity of the PDSI to the Thornthwaite and Penman-Monteith parameterizations for potential evapotranspiration. *J Geophys Res Atmos* 116(D3):D03106.
51. Taylor KE, Stouffer RJ, Meehl GA (2012) An overview of CMIP5 and the experiment design. *Bull Am Meteorol Soc* 93(4):485–498.
52. Rogelj J, Meinshausen M, Knutti R (2012) Global warming under old and new scenarios using IPCC climate sensitivity range estimates. *Nat Clim Chang* 2(4):248–253.